



Power Supply Design Seminar

Examining Wireless Power Transfer

Reproduced from
2014 Texas Instruments Power Supply Design Seminar
SEM2100,
Topic 3
TI Literature Number: SLUP321

© 2014, 2015 Texas Instruments Incorporated

Power Seminar topics and online power-
training modules are available at:
ti.com/psds

Examining Wireless Power Transfer

John Rice

ABSTRACT

Since 2009 international consortiums, including the Wireless Power Consortium (WPC), Power Matters Alliance (PMA) and more recently the Alliance for Wireless Power (A4WP), have been advancing wireless power standards for the safe, reliable and efficient transfer of power wirelessly. In this topic the principles behind wireless power are examined as well as the existing and emerging standards intent on accelerating market acceptance. The topic covers the theoretical and practical design considerations of wireless power transfer (WPT), including a study of the field behavior of loosely coupled coils, application of high Q resonant coils to overcome losses associated with poor coupling, communication between the isolated coils, foreign object detection (FOD), EMI/EMC and safety requirements imposed on electromagnetic fields.

I. INTRODUCTION

A. Wireless Power Transfer (WPT)

Wireless power is usable power transmitted over a distance and sufficient to charge a battery or power an electric circuit. The technology has been understood and applied for decades, even a transformer constitutes wireless power transfer, albeit over a very short distance. So what has changed to make this topic relevant again? In a word, it is vision, a vision that aligns and facilitates our wireless world and an “internet of things” – an infrastructure where objects in our world are uniquely identifiable and virtually represented on the Internet.

Nicola Tesla was the first to envision a world powered wirelessly. Like Tesla, Marian Soljačić of MIT envisions a world where highly tuned, resonant circuits focus energy transfer over meters of distance and deliver it efficiently to power TVs, lights and electronics. In fact, in 2007 Soljačić and his research team at MIT were able to transfer 60 W of power over 2 meters at >40% efficiency using a pair of 60 cm, helically wound coils [1].

But the application of WPT goes beyond vision and infrastructure and is often driven by pure necessity. For example, wireless power technology is often used as an alternative to wired power where electric shock, corrosion or spark ignition of explosive gases is possible and hazardous. It is also used in powering or charging surgical tools and biomedical implants where a sterile, hermetic seal is necessary. Clearly WPT is a useful and

necessary technology, but in the absence of a “killer app”, it remains largely dormant in the arsenal of power electronic care-about. Interestingly, the rebirth of wireless power is not being driven by necessity, at least not yet, but by **convenience**. The most widely deployed application for a **standard based**, wireless power infrastructure is in charging cell phones, “wearable electronics” and other internet-connected battery operated devices.

Making wireless power viable requires a deep understanding of power electronics, electromagnetic field theory and the emerging standards that help ensure the reliable, safe and efficient transfer of power wirelessly. Figure 1 illustrates one configuration where a transmit (TX) coil, wrapped around an alignment magnet, generates a time varying magnetic flux that couples to a receiver (RX) coil – electromagnetic induction. Coil separation in these applications is often less than 15 mm and magnetic shielding is necessary to contain leakage flux that otherwise reduces power transfer efficiency and causes heating in foreign and friendly metals – a friendly metal is defined as any conductive material the system is aware of, for example the alignment magnet.

Considering the number of cell phones that are shipped per year, each with a power adapter and cable, one quickly realizes the benefit of a wireless power infrastructure where the RX coil is integrated into the phone electronics and the TX coil is embedded in a mat on a kitchen counter, in

a table at a favorite coffee shop or inside an automobile passenger compartment – no adapters or cables to worry about connecting and being tethered to, no adapters or cables that often end up in landfills when you decide to update your electronics.

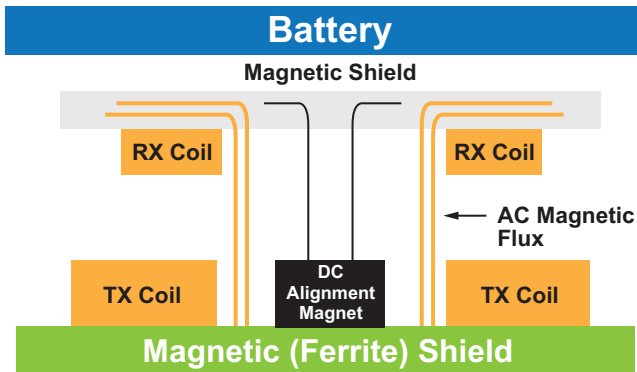


Figure 1 – Typical WPT application diagram.

As this paper demonstrates, achieving an efficient, cost effective wireless power solution is possible by careful application of familiar power electronics design theory and by using state-of-the-art wireless power technology.

i. How Much Power?

At the most basic level, the design of a wireless power transmitter is defined by the required transmit power and any requirement for spatial freedom. Spatial freedom is a term that describes the operational tolerance of a wireless power system to transfer power between coils that are separated and/or misaligned. When it comes to charging a battery, the required power is determined by battery capacity and battery chemistry. Assuming the majority of portable electronic devices use a single cel Li-Ion battery with a plateau voltage of 3.3 V and a battery capacity of under 3000 mAh, the typical power level required can be determined. Limiting the charging current of a Li-Ion battery to $\frac{1}{2}$ the battery capacity extends battery life [2]. As such, a 3000 mAh battery is charged at a maximum current of 1.5 A – a current that may be applied through most of the charging cycle. Consequently the mainstream application

for wireless battery charging is at a power level of under $1.5 \text{ A} \times 3.3 \text{ V} = 5 \text{ W}$. This is not to say that wireless power cannot or is not applied at much higher power levels. Over 20 years ago an inductive charging standard, J1773, was advanced to safely and efficiently charge lead acid batteries used in battery electric vehicles including General Motor's EV1 and the Toyota RAV4 [2]. Introduced in 1996, the Magne-Charge system, a tightly coupled system, was capable of inductively charging a battery at 6.6 kW (level 2 charging) and 50 kW (level 3) by inserting a TX paddle into a RX slot. Today wireless power systems are advancing to charge electric cars and buses at power levels exceeding 30 kW and at distances of up to 30 cm [3]. Wireless charging enables the design of electric buses with batteries that are smaller, lighter and lower cost by embedding TX coils along a street path and/or at strategic locations along a deterministic route.

ii. Foundations in Electromagnetism

The progression of knowledge in the area of electromagnetism began with the early work of Biot and Savart, Ampere and Oersted, who quantified the relationship between electric current and magnetic fields, and it progressed to the great discovery of electromagnetic induction by Michael Faraday in 1831. By 1864 James Clerk Maxwell synthesized all previous observations and in elegant mathematical form explained the full behavior of electromagnetic radiation and wave propagation. Nicola Tesla's work, most notably his work with AC power transfer, resonance and the induction motor significantly advanced the practical application of electromagnetic theory including wireless power transfer. [4]

In the world of portable electronics, biomedical implants and battery electric vehicles the idea of efficient WPT has been reborn and, since 2007, a great volume of work has been published to advance this technology. But the challenges of wireless power remain – how to safely and efficiently transfer power over a distance.

B. Near-Field vs. Far-Field – How to Transfer Usable Power

In 1909 Guglielmo Marconi won the Noble prize in physics for advancing wireless telecommunications, a form of wireless energy transfer. In telecommunication, a signal is transmitted over great distance, but the energy at the receiver needs only be large enough to distinguish it from noise – much of the energy at transmission is dispersed and lost through radiation. In contrast, making WPT practical necessitates the efficient transfer of power with minimal radiation losses over a much shorter distance.

An electromagnetic wave within a media is characterized in terms of the distance from the source and its properties in that region, i.e. which fields dominate and how quickly they decay. These properties are illustrated on the wave impedance plot shown in Figure 2. The red trace represents the impedance of a dipole antenna and the blue trace a loop antenna similar to what is used in inductive wireless power transfer. The product of r_c and β is proportional to the wavelength and representative of the distance from the source.

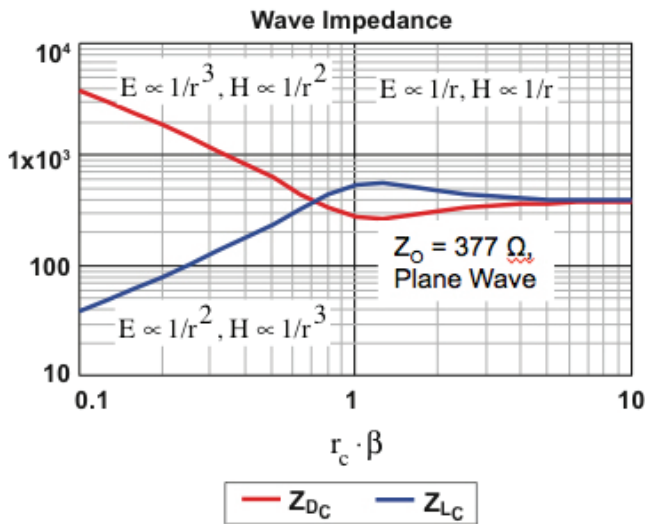


Figure 2 – Wave impedance of a dipole and loop antenna.

Wave impedance is the ratio of the electric field in V/m to the magnetic field in A/m. In the far-field, where the $r_c\beta \gg 1$, the electric and magnetic field impedances converge and approach

the impedance of free-space, Z_0 , a constant of 377 ohms. In this region magnetic and electric fields behave the same regardless of the source (antenna). Where one defines the “near-field” is somewhat subjective, but is generally accepted to be below one wavelength from the transmitting antenna. The reactive near-field occurs at and below a fraction ($1/2\pi$) of a wavelength and is a non-radiative storage field – this is the region of most interest for inductive wireless power transfer. In this region the H-field and E-Field are strong and out of phase by 90 degrees producing a reactive impedance [5]. A dipole antenna produces a wave impedance much greater than Z_0 in the reactive near-field because E is much greater than H. Similarly, a loop antenna produces a wave impedance that is much less than Z_0 because H is much greater than E in this region.

Usable wireless power is accomplished in the far or near field as illustrated in Figure 3. Far-field energy radiates (and disperses) through space and the received power varies inversely with the square of the distance from the source. In the far-field, microwave and lasers have been used to transfer significant power over great distance using high directivity antennas or well collimated laser beams – power beaming. However, the practical application of far-field radiation for transferring power over great distances is beyond the scope of this paper. Instead, this topic focuses on inductive power transfer that occurs at a small fraction of the transmit wavelength in the reactive near-field, where the magnetic field strength is strong but falls off at a rate proportional to the inverse cube of the distance from the source. This, combined with safety restrictions imposed on electromagnetic fields, typically limits the practical application of wireless power to a few meters. As presented shortly, magnetic induction (MI) and magnetic resonant (MR) represent the most efficient methods of transferring any significant amount of power wirelessly.

Where MI may operate over a relatively wide range of frequencies, MR typically operates near or at resonance [6]. In wireless power terminology the terms “loosely coupled” and “tightly coupled” coils are often used to differentiate MI from MR. But, in this context, “tightly coupled” is a reference to coil proximity more than flux coupling and is

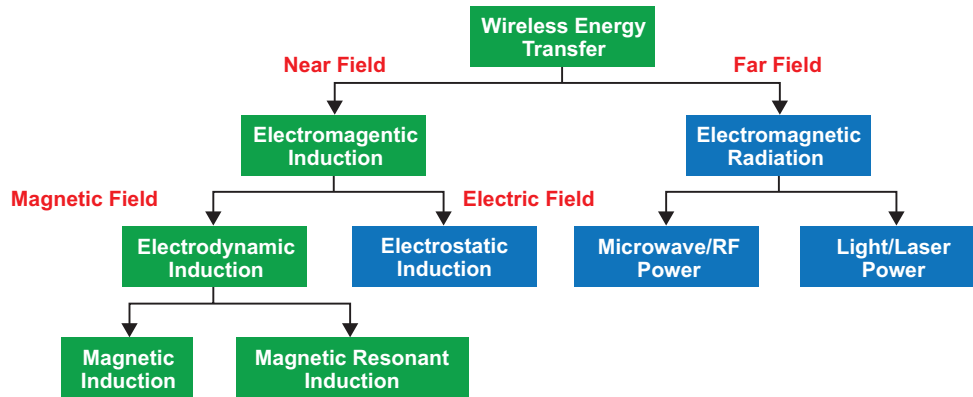


Figure 3 – Wireless energy transfer technologies.

misleading when compared with a transformer where the coupling coefficient, a measure of how tightly a coil pair is flux coupled, is nearly 1. In terms of the coupling coefficient, the practical operating range for MI is between 0.8 and 0.3 – MR extends this range down to less than 0.01.

C. A Race to Standardize Wireless Power

The current vision and projection for a wireless power infrastructure necessitates a certification standard. Certification enhances consumer confidence and helps ensure product safety and reliability. Since 2009 international consortiums have been looking to advance a robust wireless power standard that accelerates market acceptance. A key advantage of being standards compliant or compatible is product interoperability – a term that describes the ability of any certified transmitter to communicate with any certified receiver. Presently there are three evolving standards as of the writing of this paper. The Wireless Power Consortium Qi (energy) standard is the most developed with over 200 member companies, hundreds of products and 50 M devices already in the market. The WPC also has endorsement by the Consumer Electronics for Automotive (CE4A), an organization working with European

automakers to standardize mobile interfaces [7]. Another consortium of companies, the Power Matters Alliance (PMA), advances inductive wireless power technology that is similar in operation to the WPC Qi standard. In fact, so called “dual mode” receivers and transmitters are available that support both standards [8]. Leveraging corporate relationships with General Motors, Starbucks, AT&T and others, the PMA is positioned to participate in the explosive growth in wireless power. The last wireless power standard, the Alliance for Wireless Power (A4WP), now called Rezence, appeared in 2012 proposing magnetic resonance for greater coil separation and spatial freedom. Notable differences between the standards are illustrated in Table 1. While the WPC and PMA operate between 100 and 400 kHz the A4WP standard operates at the low end of the ISM band at 6.78 MHz. Another key difference is in how the receiver communicates with the transmitter to facilitate load regulation. Where the WPC and PMA both communicate with the transmitter using secondary side load modulation over the same forward power path, the A4WP requires a secondary wireless communication technology – typically Bluetooth Low Energy (BLE), Zigbee or WiFi.

| Products | Power Frequency Band | Communication Frequency Band | Range of Coupling |
|------------------------------------|----------------------|------------------------------|-------------------|
| Wireless Power Consortium (WPC) | 105-205 kHz | Same as power transfer band | 0.4 to 0.7 |
| Powermat (PMA) | 277-357 kHz | Same as power transfer band | 0.6 to 0.8 |
| Alliance for Wireless Power (A4WP) | 6.78 MHz | 2.4 GHz (ZigBee or BLE) | 0.1 to 0.5 |

Table 1 – Existing WPT standards.

Initially targeting cell phone battery charging, WPT technology has evolved from wireless power “receiver sleeves” that slip onto an electronic device to fully integrated solutions where the receiver is designed into the electronic device. Verizon, Samsung, Nokia and others all have advanced phones with integrated wireless receivers.

D. Safety Matters – Limiting Field Exposure

How electromagnetic fields affect health is an important consideration in advancing any wireless technology, wireless power included. In the United States many follow guidelines set by the IEEE C95.1 standard, whereas Europeans generally adhere to stricter guidelines imposed by the International Commission on Non-Ionizing Radiation Protection (ICNIRP). As Figure 4A illustrates, the electromagnetic spectrum includes non-ionizing radiation, which extends from DC to visible light and ionizing radiation including ultra-violet, x-ray and gamma-rays and other high energy radiation that has enough energy to alter or break DNA bonds. Figure 4A also illustrates the separation point between ionizing and non-ionizing radiation and where wireless power is typically employed. In order to protect against known health effects, these agencies publish

guidelines for maximum exposure differentiating between general public and occupational limits [9]. Guidelines like the one shown in Figure 4B exist for magnetic (H-field), electric (E-field) and current density fields (J-fields).

The guidelines are based on an extensive number of related scientific publications and volunteer studies and have been reviewed by dozens of national expert committees. The ICNIRP states that based on these studies: “There is no substantive evidence that adverse health effects can occur in people exposed to levels at or below the ICNIRP limits.” That said, consideration of these limits should be considered carefully by anyone hoping to transmit significant amounts of power using electromagnetic fields. Take for example the ICNIRP guidelines at 10 MHz. The guideline indicates that at 10 MHz the general public should not be exposed to magnetic fields in excess of 0.073 A/m or electric fields greater than 28 V/m. According to their 2007 Science paper [10], Soljačić and his colleagues measured a magnetic field of 1 A/m at halfway between TX and RX coils—nearly 14 times the ICNIRP limit. The electric field was 210 V/m, which exceeds the ICNIRP limit by a factor of 7.5. Twenty centimeters away, the magnetic field was more than 100 times and the electric field 50 times the ICNIRP limits.

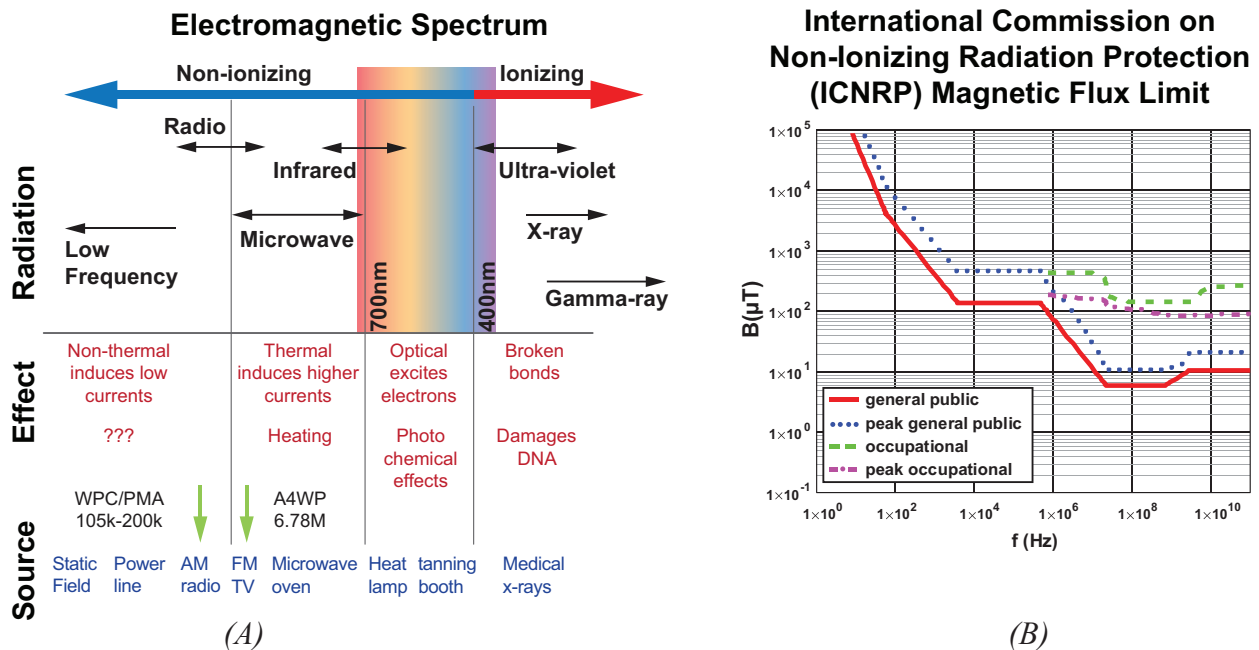


Figure 4 – The electromagnetic spectrum safety considerations.

II. THEORY OF OPERATION

A. Maxwell's Equations

The theory behind WPT is explained using Maxwell's equations, shown in integral form in Figure 5. These equations relate everything currently known about electric and magnetic field behavior. They include Gauss's laws for electric and magnetic fields, Faraday's law and the Ampere-Maxwell law. The Ampere-Maxwell equation is a transverse wave equation where the velocity of the wave is exactly the speed of light and directly related to the permeability (μ_0) and permittivity (ϵ_0) of free space. From Faraday's law of induction (Maxwell's third law) it is understood that a changing magnetic flux in a coil induces a voltage in that coil such that the field produced opposes the field that generated the voltage in the first place. This is Lenz's law and it is true for any magnetically coupled coil pair. Coils used in wireless power transfer are generally separated and/or horizontally misaligned – either displacement negatively affects the percentage of flux that couples between the coils and significantly limits the amount of energy that is transferred efficiently. Hence, the challenge of wireless power is to come up with an efficient way to transfer energy through low permeable air between two coils that are not necessarily in close contact or center aligned.

$$\oint \mathbf{E} \cdot d\mathbf{A} = \frac{\Sigma Q}{\epsilon_0}$$

$$\oint \mathbf{B} \cdot d\mathbf{A} = 0$$

$$\oint \mathbf{E} \cdot d\mathbf{l} = -\frac{d}{dt} \oint \mathbf{B} \cdot d\mathbf{A}$$

$$\oint \mathbf{B} \cdot d\mathbf{l} = \mu_0 i_{enc} + \mu_0 \epsilon_0 \frac{d}{dt} \oint \mathbf{E} \cdot d\mathbf{A}$$

$$\mu_0 = \text{Vacuum_permeability}$$

$$\epsilon_0 = \text{Vacuum_permittivity}$$

Figure 5: Integral form of Maxwell's equations.

B. Magnetic Link Efficiency

The mutual inductance of a pair of current-carrying coils is proportional to the amount of magnetic flux linkage between them. It is mathematically expressed in terms of the individual coil self-inductances and the coupling coefficient (k) as shown in Equation 1 and graphically as in Figure 6. Clearly the flux generated by the transmitter and the flux captured by the receiver is related to the coil arrangement and geometries, but is also influenced by the materials used to make the coils.

$$M = k\sqrt{L_1 L_2} \tag{1}$$

Like a transformer, the flux generated by the transmitter (primary) is proportional to the ampere-turns (A-T) in that coil. Unlike a transformer where the coupling coefficient, k , is nearly 1, k is typically between 0.1 and 0.8 in wireless power applications – a direct result of coil separation, coil misalignment and the materials used to build the small, cost effective coils used in consumer electronics. The electrical representation for the voltage induced in the secondary is shown in Figure 6 where the induced voltage, V_2 , is a function of the mutual inductance and the rate of change in current of coil 1.

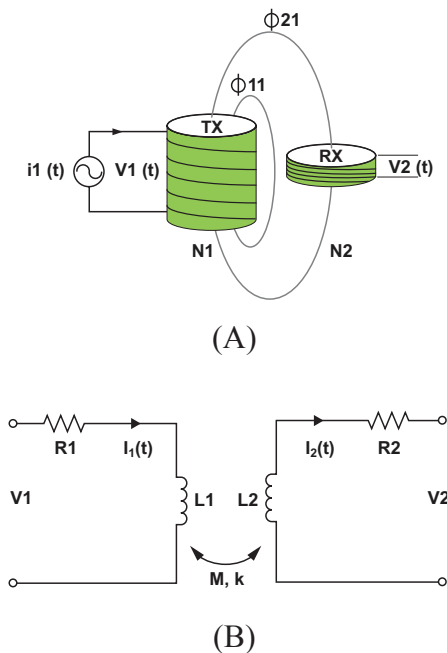


Figure 6 – Graphical (A) and electrical (B) illustration of mutual inductance.

The induced voltage is also opposed by the rate of change of current in coil 2 and any resistance, AC or DC, in series with it. Making a wireless power transfer system efficient is then largely about optimizing flux coupling and canceling leakage inductance through resonant power transmission.

C. Circuit Model of a WPT

The wired transfer of power from a voltage source to a load is well-understood and easily quantified using Kirchhoff's voltage and current laws. Losses in the interconnect wires and source impedance are generally negligible compared with the power delivered to the load. The analysis extends to isolated power transfer, as in Figure 7. Using an ideal transformer the voltage at the secondary is transformed by the ratio of the number of turns on the primary and secondary coils. In this configuration the coupling between the primary and secondary is considered to be ideal with no winding or transformer core losses. The power seen at the secondary is then the same as in the wired application transformed by the ratio of the secondary and primary turns squared.

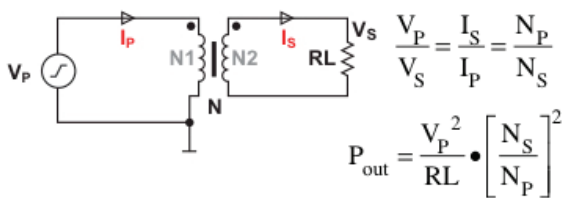


Figure 7 – Power transfer model of an ideal transformer.

Things get more interesting moving from an ideal transformer to loosely coupled inductors. A non-ideal transformer with coupled inductors can be represented as a leakage inductance and magnetizing inductance transformed using the cantilever model as shown in Figure 8.

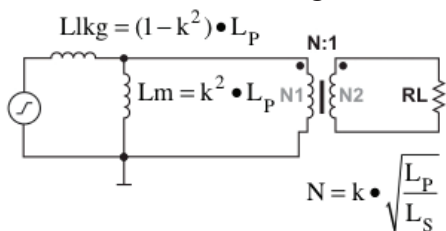


Figure 8 – Cantilever transformer model with non-ideal coupling.

The leakage and magnetizing inductances are expressed mathematically in Figure 8 and are a strong function of the non-unity coupling coefficient, k . The magnetizing inductance quickly diminishes with decreasing k forcing a greater A-T and associated losses to support a given load. The leakage inductance, shown on the primary side impedes power transfer and goes up exponentially with a reduction in k . Likewise, the turns ratio N decreases with k and is represented by the square root of the primary and secondary inductances multiplied by the coupling coefficient. Reflecting the load to the primary using N , the effective load resistance seen by the primary becomes very small as k decreases.

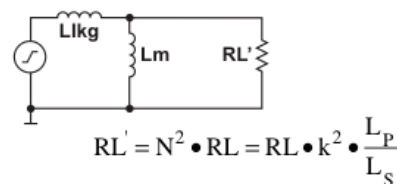


Figure 9 – Secondary load reflected to primary.

Collectively, a poor coupling coefficient works against wireless power transfer by increasing source impedance and reducing reflected load impedance. Hence, impedance cancelation of the distributed leakage inductance and loss mitigation with high Q coils is what makes the wireless transfer of usable power possible.

D. Resonance to the Rescue

In wireless power, series or parallel resonance must be applied to overcome the effective leakage inductance associated with poor coupling [11] [12]. For battery charging applications, a secondary parallel resonant circuit works well as this appears to the battery as a current source. The leakage inductance, L_{lk} in Figure 10, is in series resonance with $C2$. At resonance the reactive impedance of the inductor cancels the reactive impedance of the capacitor, essentially connecting the source to the load. $C3$ is in parallel resonance with L_m . A defining and critical characteristic of any resonant wireless power design is the circuit quality coefficient, Q . As shown later in this paper, a high Q mitigates losses coincident with poor coupling and helps improve power transfer efficiency. Q is a dimensionless number that is expressed in

several ways, but fundamentally relates the reactive losses of a component or circuit tank to the real losses.

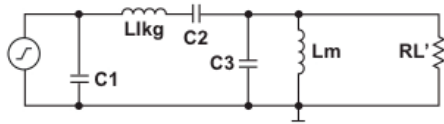


Figure 10 – Applying resonance to cancel effective leakage.

$$Q = 2 \cdot \pi \cdot \frac{\text{Energy Stored}}{\text{Energy dissipated per cycle}} = \frac{2 \cdot \pi \cdot f_r \cdot \text{Energy Stored}}{\text{Power Loss}}$$

The unloaded Q of a coil is easily measured on a vector network analyzer (VNA) using a single port measurement. In a single port measurement, the VNA variable frequency oscillator is applied directly to the coil to measure coil impedance, from which the resonant frequency and bandwidth are also determined [13]. The family of curves in Figure 11 was plotted in SPICE for a typical WPC TX series resonant tank. The resonant waveform in Figure 11 is defined by the 3 dB points on the right and left side of resonance from which Q can be calculated.

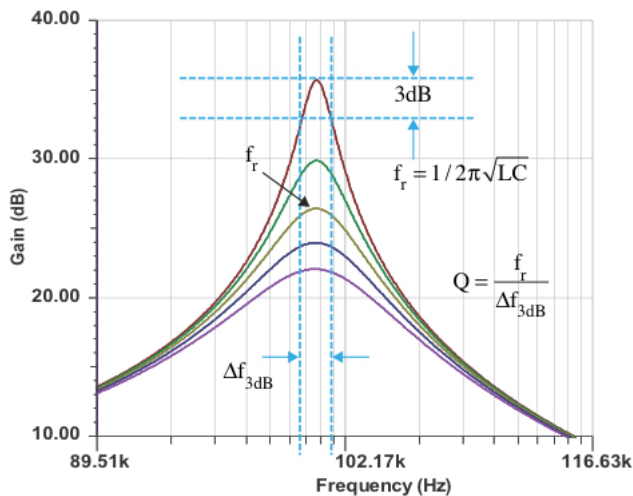


Figure 11 – Resonant frequency and Q of a resonant tank.

The circuit behavior of a wireless power transmitter can be modeled in SPICE if the combined coil impedance is known, but AC losses

are frequency dependent, so modeling the coil behavior is not trivial [14]. By definition, a high Q wireless power converter facilitates lower losses and greater spatial freedom, but operating near or at resonance with high Q coils requires higher control precision and bandwidth. As a general rule-of-thumb, the precision of frequency tuning for a magnetic resonant control is proportional to $1/Q$ – the higher Q, the greater the required precision of frequency. As with any resonant control topology, the option for input voltage modulation at a fixed frequency is also available. This method is generally employed when EMC concerns restrict the frequency band of operation.

E. Transmit and Receive Coil Losses

Just as winding losses of a transformer must be considered carefully, the AC winding losses of a wireless power converter’s coupled inductor pair must also be considered. To achieve good transfer efficiency one must address coupled inductor skin and proximity effects. As seen in Equation 2, using high Q coils can minimize coil losses associated with frequency dependent AC winding resistances. Because the A-T in the TX increase exponentially with smaller k, the Q of the TX is generally more important in mitigating losses. Typically a 5 W TX coil has an unloaded Q between 50 and 100, but making a high Q coil is expensive, so trade-offs must be made, especially in consumer electronics intended for portable applications where both coil size and cost matter.

$$R_p = \frac{\omega \cdot L_p}{Q_p} \quad R_s = \frac{\omega \cdot L_s}{Q_s} \quad (2)$$

With a goal of achieving good efficiency and an understanding that the most widely deployed applications for wireless power are under 5 W, it is worthwhile to quantify the Q and AC resistance of a typical 5 W coil pair.

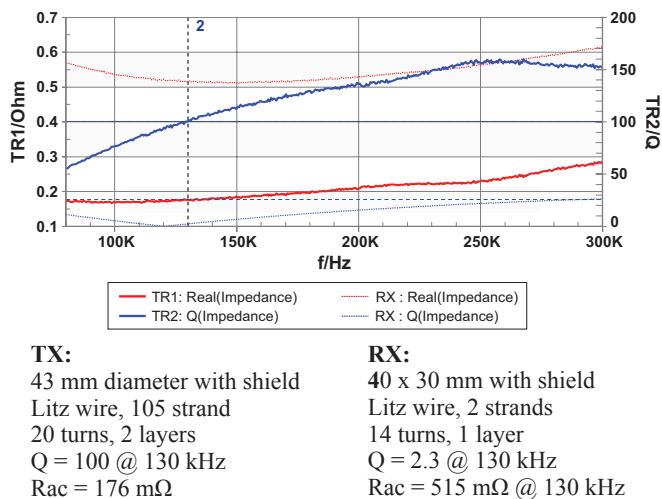


Figure 12 – TX and RX coil impedance and Q, unloaded.

Figure 12 illustrates the typical coil impedance of an RX and TX coil pair used in a 5 W application. The TX coil has 20 turns, 2 layers and 105 strands of Litz wire and a diameter of 43mm. The unloaded Q of this coil is measured to be 100 at 130 kHz and has an AC winding resistance of 176 mOhms. The RX coil measuring 40 x 30 mm is typical of what might be integrated into a cell phone “sleeve”. It is bifilar wound with 2 strands and 14 turns and has a Q of 2.3 and an AC winding resistance of 515 mOhms at 130 kHz. In a typical 5 W application, the system Q is relevant to efficiency and is a geometric mean of the two coils. As previously mentioned, high Q coils are expensive, but they can also be large, so for high volume, portable electronics the determination needs to be made when “good is good enough”. Later in this paper it is shown that this coil pair is sufficient to achieve system efficiencies close to 80% at a 5 W output.

F. Predicting Primary Current as a Function of the Coupling Coefficient, k

The primary tank circuit of a wireless power transmitter is driven by trapezoidal waveform at 50% duty cycle similar to an LLC power converter topology.

Primary winding losses increase by the square of the primary current and exponentially as the coupling coefficient decreases. Unless high Q

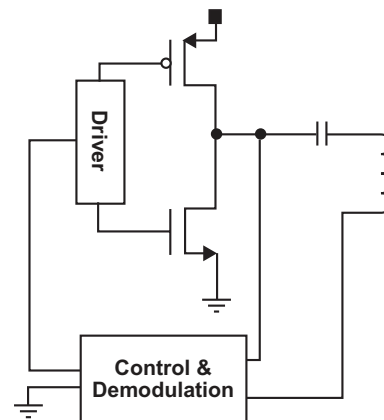


Figure 13 – TX side 1/2 bridge power stage and control.

coils are used, particularly on the TX coil, AC winding losses not only result in poor power transfer efficiency, but can also impact reliability and safety. For example, in battery charging applications with “tightly” coupled coils the battery may be thermally coupled with the TX coil. Therefore, losses in the TX winding must be managed carefully, especially in applications operating at elevated ambient temperatures to avert reliability and safety issues associated with elevated battery temperatures.

To quantify how primary current and operating frequency varies with load, coupling coefficient and Q a first harmonic approximation (FHA) method of the trapezoidal voltage is presented here. The cantilever model previously developed is also used in this AC analysis. The circuit leakage and magnetizing inductance have previously been defined (Figure 8) in terms of the coupling coefficient, and the turns-ratio is determined based on measured coil inductances. The resonant components are selected based on the input voltage and operating frequency range and an impedance transformation is applied to reflect the secondary impedance to the primary [15] [16]. The input voltage in the analysis is set at 19.5 V from which we get an FHA fundamental voltage of $2 \cdot 19.5 / \pi = 12.4$ V. The resonant tank current is expressed in terms of the fundamental voltage and calculated complex input impedance, Z_{in} , using the cantilever circuit model and Q transformation described earlier.

$$i_r(f, k) := \frac{V_{\text{fundamental}}}{Z_{in}(f, K)} \quad (3)$$

$$Z_{in}(f,k) = R_p + \frac{R(k) \cdot Q_p(f,k)^2}{1 + Q_p(f,k)^2 \cdot \frac{XC(f,k)}{XL_p(f,k)}} + j \cdot \frac{XL_s(f,k) - XC_r(f) + \frac{R(k) \cdot Q_p(f,k)^2 \cdot XC(f,k) \cdot 1 - \frac{XC(f,k)}{XL_p(f,k)}}{1 - Q_p(f,k)^2 \cdot 1 - \frac{XC(f,k)}{XL_p(f,k)}}}{2} \quad (4)$$

$Z_{in}(f,k)$ is derived with the Q-transformation and cantilever model previously discussed, as shown in Equation 4.

Figure 14A and B represent the predicted behavior of a 5 W wireless power transmitter. From Figure 14A with $k=0.6$ it is seen that a 1 A output current corresponds with an operating frequency of 163 kHz, consistent with measurement. If the tank is run at 163 kHz, the corresponding resonant current from Figure 14B is 1.43 A and the input current is equal to $(5W/eff)/V_{fundamental}=0.4A$. This assumes a modest conversion efficiency of 70%. From the expression in Equation 4, if k is reduced to 0.3, the resonant tank frequency moves closer to resonance and the current increases to 2.5 A. Clearly the increased amper-turns further increases losses associated with AC and DC winding resistance unless high Q coils are used.

G. Coil Coupling Efficiency

The “flux net” of a receiver is intuitively a function of the coil diameter; the bigger the coil the more flux captured by an RX or generated by a TX to induce voltage. Often the RX coil needs to be made as small as possible to accommodate a product’s form-factor at the expense of power transfer efficiency. The family of curves in Figure 15 relates the efficiency of a coil pair to the coil diameters and vertical displacement where the displacement is normalized to the TX coil diameter. Take for example an RX coil that is equal to the transmit coil (red curve). If the vertical separation is 1 TX diameter (1 on the horizontal axis), then the magnetic efficiency based on flux coupling is approximately 60%. Note that this is not the power transfer efficiency, but rather an indication of flux linkage. Note also that the family of curves varies with Q, so higher Q resonant circuits afford greater flux linkage and ultimately higher efficiency.

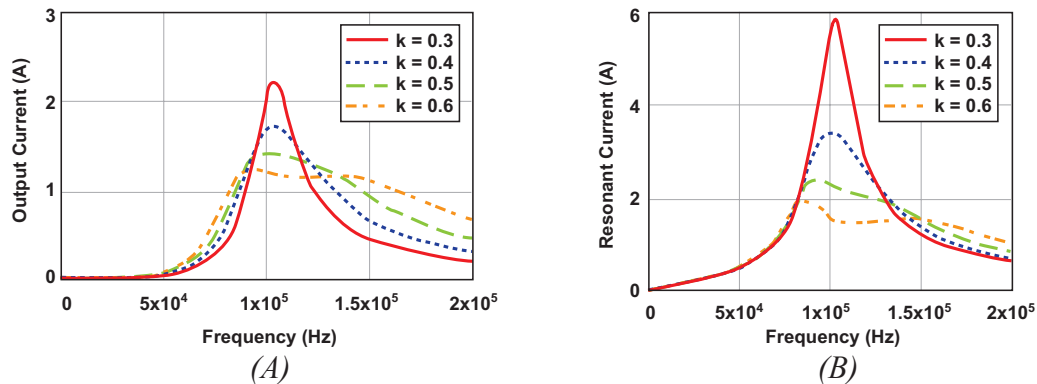


Figure 14 – RX and TX coil current.

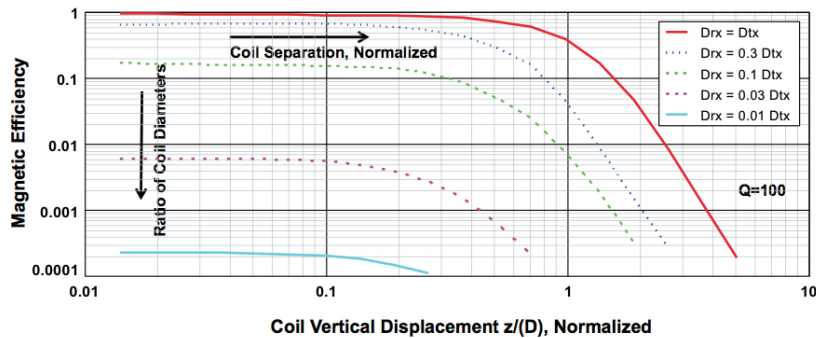


Figure 15 – Magnetic flux coupling as a function of Q, coil geometries and displacement.

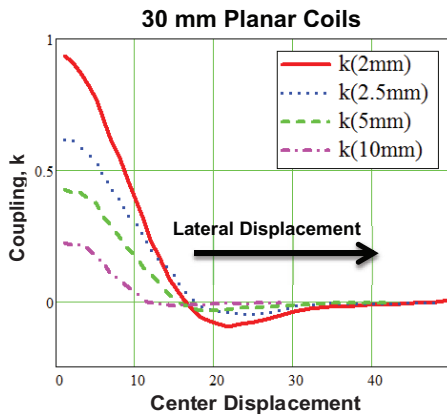


Figure 16A – 30 mm coil pair k relative to vertical and lateral displacement.

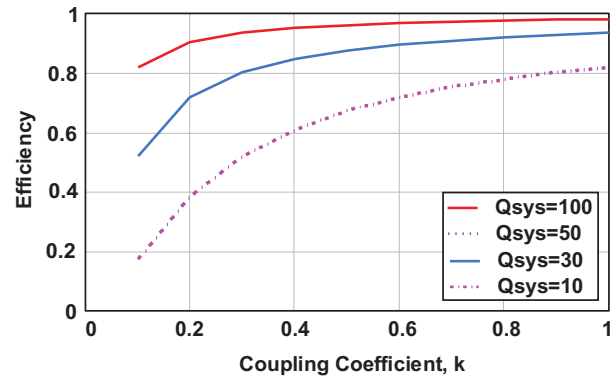


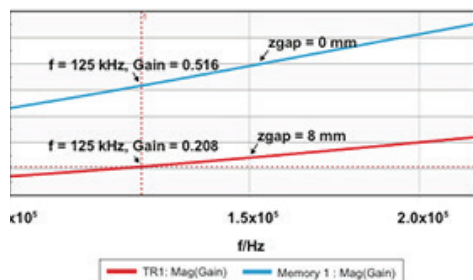
Figure 16B – Transfer efficiency relative to system Q .

H. Coupling Efficiency

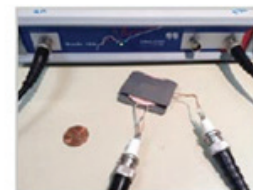
To further investigate the effect of the coupling coefficient on efficiency consider the graphic in Figure 16A. The graph measures the coupling coefficient of two 30 mm coils with vertical and lateral displacement. The horizontal axis represents a lateral displacement from center alignment and each curve represents a separate measurement of vertical displacement. For example, the lowest dashed line represents a 10 mm vertical coil displacement and $k = 0.38$ when the lateral displacement equals 0 mm – center alignment. Adding 10 mm of lateral displacement reduces k from 0.35 to 0.2. The graphic in Figure 16B represents the theoretical magnetic efficiency and how a higher Q compensates for poor coupling. For example, the magnetic figure of merit of a system with a Q of 100 and a $k = 0.2$ has a flux coupling efficiency $>80\%$.

I. Measuring Mutual Inductance and the Coupling Coefficient

The transfer gain of a pair of unloaded, coupled inductors can be measured using a vector network analyzer (VNA). Figure 17 illustrates the setup and measurement of a typical 5 W coil pair; notice that the coils are in close vertical and center alignment. Using the oscillator port of the VNA and one of the channels to plot the transfer gain, k is calculated indirectly from this using the measured coil inductances. The RX coil (top) has 14 turns and is bifilar wound. The TX coil (bottom) has 20 turns and uses 105 stranded Litz wire. The WPC defines an operating frequency between 105 kHz and 205 kHz, so at a frequency of 125 kHz the converter is heavily into resonance. The coils are measured with a 0 mm gap and an 8 mm gap and the corresponding coupling coefficients and mutual inductance are calculated from this plot and are shown in Figure 17. Notice that as the gap increases from 0 mm to 8 mm the mutual inductance drops by over 50% from 13.6 μH to 5.27 μH .



$$k = \sqrt{\frac{L_{rx}}{L_{tx}}} \cdot \frac{V_{tx}}{V_{rx}} = \frac{\text{Gain}}{\sqrt{\frac{L_{rx}}{L_{tx}}}}$$



Typical 5 W coils connected to a VNA

$$k(\text{gap} = 0 \text{ mm}) = \frac{0.516}{\sqrt{\frac{L_{rx}}{L_{tx}}}} = 0.83, M = 13.6 \mu$$

$$k(\text{gap} = 8 \text{ mm}) = \frac{0.208}{\sqrt{\frac{L_{rx}}{L_{tx}}}} = 0.321, M = 5.27 \mu$$

Figure 17 – Transfer gain.

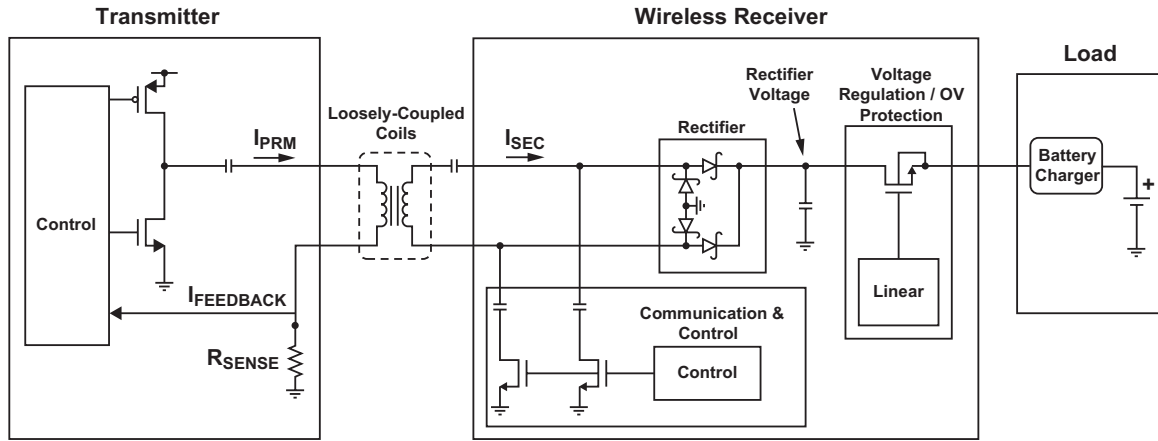


Figure 18 – Typical 5 W WPT architecture.

J. Architecting a WPT Transmitter

As stated earlier, the circuit architecture of a wireless power transmitter depends fundamentally on the required power level and coil separation/alignment. Other care-about include standards compliance and specified end user requirements including source voltages and possible keep out frequencies. The power stage driving the TX coil must be a resonant topology to achieve respectable efficiency. This requires a frequency modulated power architecture where the operating frequency of the resonant tank is dependent on line and load changes. It is also possible to modulate the input voltage and maintain a fixed frequency [17]. In Figure 18 the transmitter is a series resonant coil driver in a 1/2 bridge topology operating at 50% duty cycle, much like an LLC converter. The receiver is a tuned resonant circuit that magnetically couples the primary flux, rectifies the induced AC voltage and conditions it. As far as wireless power is concerned, that is about it. Now suppose the need arises to communicate with the primary while remaining wireless. One approach is to intelligently modulate the load such

that the load impedance is reflected to the primary as a modulated voltage and current; these can then be demodulated by the TX and interpreted. According to the WPC and PMA specification, communication from the RX back to the TX uses the same magnetic coupling path as the forward power transfer. The RX side load modulation can use either a resistive or capacitive modulation. Capacitive modulation is lossless on the secondary, but does show up as an increased modulation loss term on the primary.

K. Modeling Circuit Behavior in SPICE

A simplified SPICE open loop analysis of a wireless power converter with resonant coupled inductors is presented in Figure 19. The components are selected for a typical 5 W application. The frequency domain plot shown in Figure 20A represents the transfer gain as a function of frequency and coupling coefficient, k . Lower k values result in lower operating frequencies closer to resonance for the same output power. Like an LLC converter, operation is always above the resonant frequency to facilitate

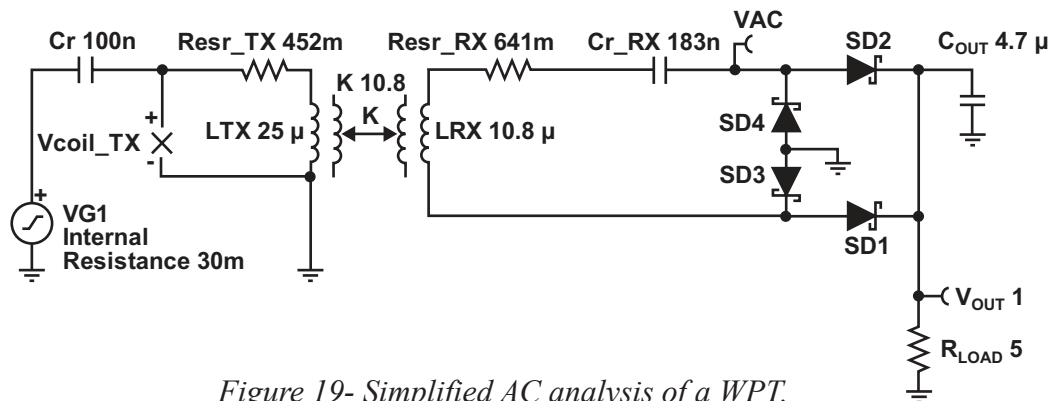


Figure 19- Simplified AC analysis of a WPT.

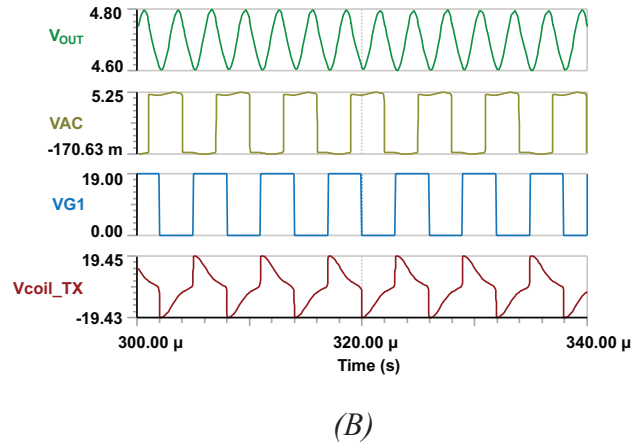
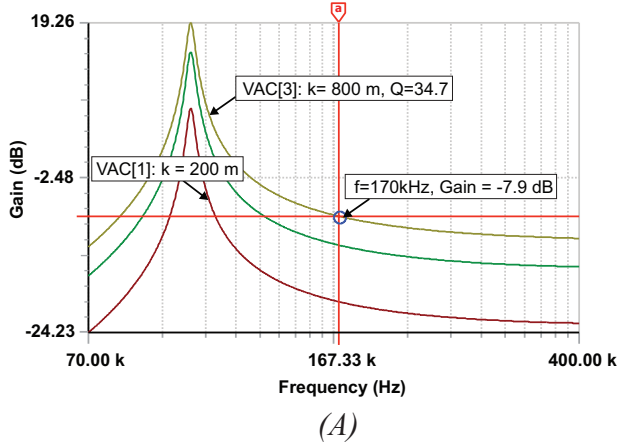


Figure 20 – Frequency (A) and time domain (B) plots of WPT.

zero volt switching (ZVS) and allow for the lowest possible inductance. At resonance the primary and secondary output voltages reach their maximum value, which can be substantial depending on the circuit Q. As frequency is increased above the resonance point, the primary/secondary amplitudes decrease. The AC simulation illustrates the typical operating range of a WPC solution where the required gain is calculated based on an input voltage of 19 V. The gain is simply $20 \times \log(V_o/V_{in})$ which corresponds to -7.9 dB on the gain transfer plot at an AC secondary voltage, VAC, of 7.65 V. This corresponds with an operating frequency of 170 kHz for the components selected. To examine behavior in the time domain, VG1 is modified to be a 19 V square wave with an operating frequency of 170 kHz and a 50% duty cycle. The same circuit can now be used to generate the time domain plot in Figure 20B. Notice that coil voltage is quasi-sinusoidal and the output voltage is 4.5 V when loaded by a 5 Ohm resistor. In an actual implementation the receiver sends communication packets back to the TX

reporting the regulation point and received power. The transmitter then adjusts the switching frequency to deliver the appropriate power.

L. Examining Behavior in the Time Domain

One of the more challenging aspects of designing a wireless power transmitter is in comprehending coil currents and voltages as a function of the coupling coefficient and associated mutual inductance. Although not appropriate for modeling load step response, the simplified open loop simulation in Figure 21 is effective in comprehending circuit waveforms and stresses in the time domain. The model is also used to examine input current harmonic content and conducted emission implications if the LISN is modelled [18]. The simulation uses a SPICE model of a gate driver with dead-time to drive a half bridge resonant tank. The frequency is controlled by any pulse source or a voltage-controlled oscillator (VCO).

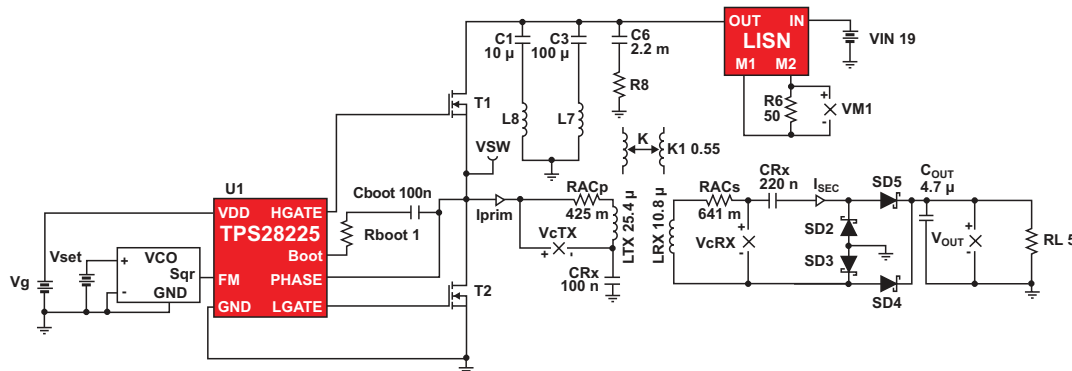


Figure 21- Time domain model of a 5 W power transmitter.

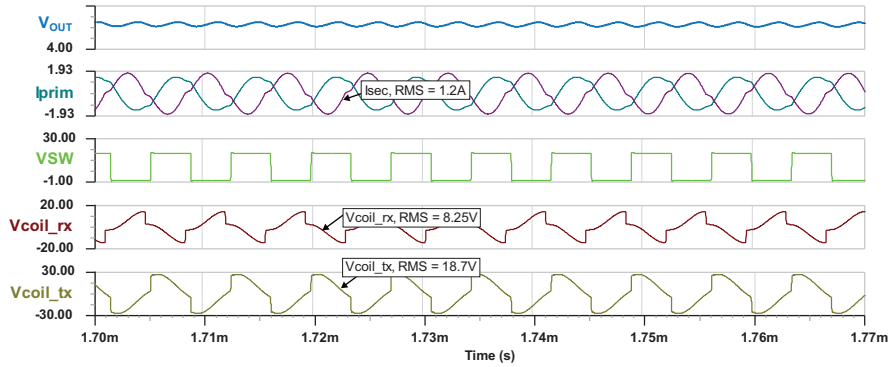


Figure 22 – Time domain waveforms of a 5 W WPT.

Note the quasi-sinusoidal behavior of the RX and TX coil voltages in Figure 22, whereas the resonant current in the tank is more sinusoidal. As the converter operating frequency moves closer to the tank resonant frequency voltages increase and become more sinusoidal.

M. Using Finite Element Analysis to Examine Field Behavior and Losses

Using Finite Element Analysis (FEA) one can visualize the electromagnetic field behavior influenced by shielding materials, coil windings materials and geometries and other influences. This provides a deep insight into wireless power and how it is optimized. This 2D analysis uses a free software package called FEMM [19]; the software is easy to configure and versatile in analyzing field behavior. The axisymmetric simulation shown in Figure 23 comprehends all the significant physical parameters of the TX and RX coils and shielding material. The power dissipation associated with AC skin and proximity effects is simulated to be 320 mW at an output power of approximately 5 W, corresponding closely with measured results.

N. Quantifying Losses

Principal losses on the transmit side include AC winding losses in the TX coil, bridge driver and power stage conductive and switching losses, control logic and any overhead associated with control side DC-DC power conversion. Receiver side losses include the AC winding losses of the RX coil, AC rectifier conduction and switching losses and post regulation (LDO) losses that are mitigated using intelligent voltage positioning as explained later. Losses are also associated with load modulation, but if capacitor load modulation is used the losses are seen on the primary as a reflected load impedance and not on the secondary. Optimal efficiency is realized using multi-stranded Litz wound planar coils. PCB coils may be fabricated for both the TX and RX, however these coils cannot perform as well as helically wound coils. Typically, size and cost are more relevant to the RX where AC winding losses are also lower. A typical 5 W planar TX coil wound with 105 stranded Litz wire achieves an efficiency of > 80% using MI. Compared with a PCB coil, expect a 10-20% hit in efficiency at 5 W depending on the WPT technology used.

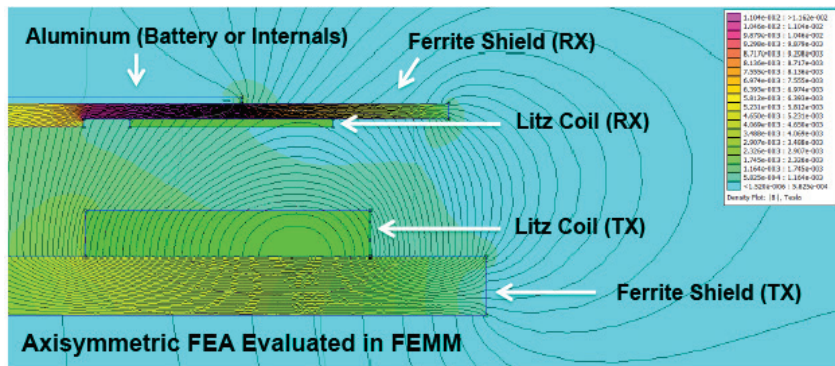


Figure 23 – Axisymmetric FEA of a 5 W coil pair.

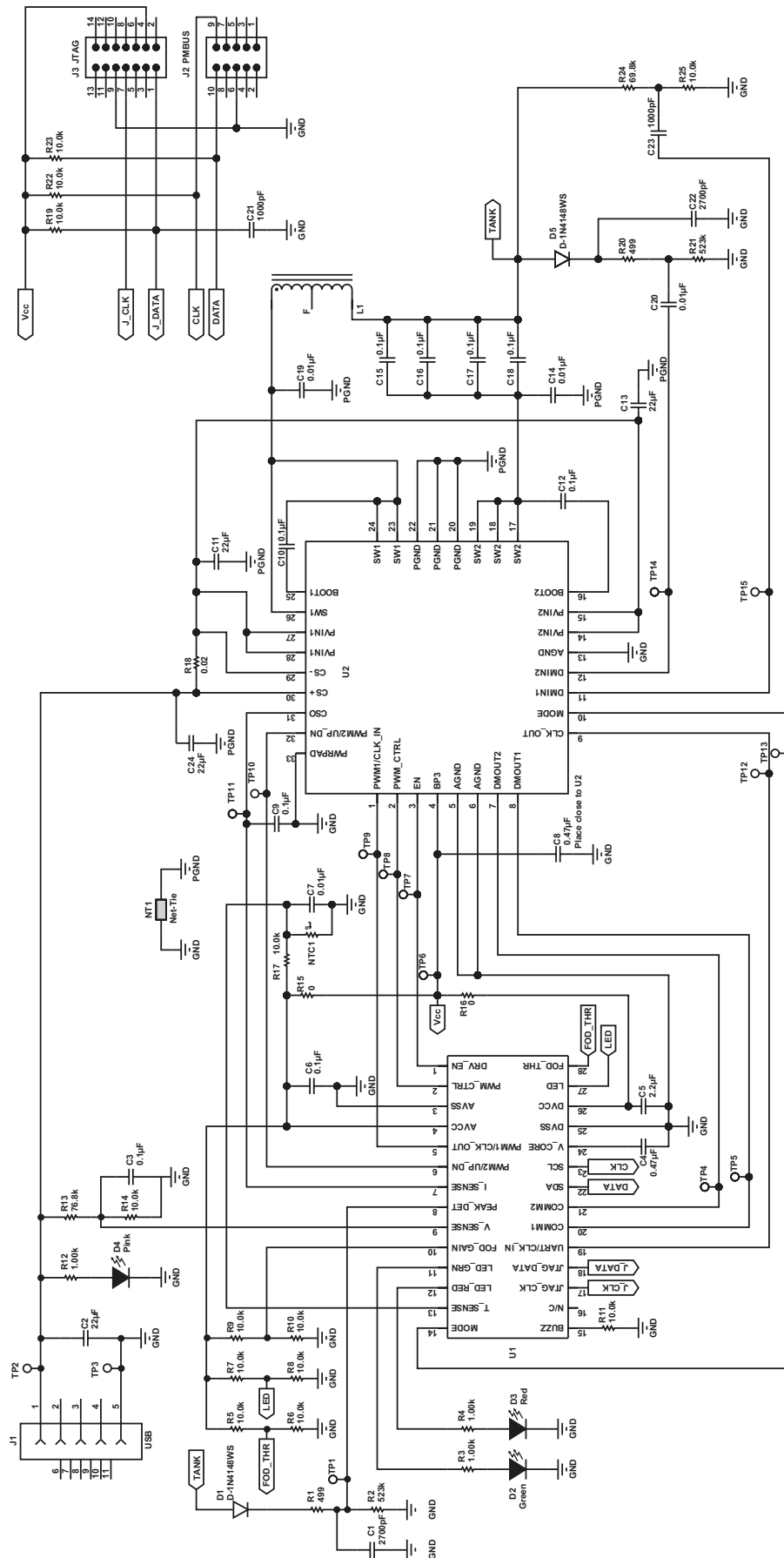


Figure 24 – Complete TX, 5 W power transmitter solution.

III. DESIGNING A WIRELESS POWER TRANSMITTER

Practical design considerations of implementing a WPT solution are examined next. Compliance with a WPT standard is not necessary, but it does have advantages including coil optimization, built-in foreign object detection and optimal EMC compliance. Another key advantage to standards compliance is marketability and interoperability.

A. Circuit Configuration and Integration

Developing a cost effective solution for wireless power that is also compliant with a standard necessitates a high level of integration and understanding of the principles presented in this paper. The two chip TX reference design shown in Figure 24 includes a microprocessor for frequency modulation and communication with the RX as well as an intelligent, highly integrated coil driver that facilitates demodulation of the RX side load modulation. The solution is capable of delivering 5 W to any WPC Qi compliant RX.

B. Communication Protocol

The communication protocol from the RX to the TX uses the same magnetic coupling path as the forward power transfer. A simple load modulation method is used to communicate status and commands back to the TX side controller. When the RX circuit is placed in proximity to a compliant TX, the TX generates a magnetic field sufficient to power the RX. The TX waits until its field is perturbed by the RX and then extended communication begins. The resulting amplitude modulation of the primary coil voltage/current is detected and demodulated by the TX. The RX then reports the required power and the TX adjusts the operating frequency to facilitate the need. The RX load modulation uses either a resistive or capacitive load element. If feedback is lost the power transfer is interrupted.

The RX microcontroller has control of two load switches and uses them to implement a “differential bi-phase” bit-encoding scheme. The TX demodulates the resulting amplitude modulated signal using analog filters or digital demodulation.

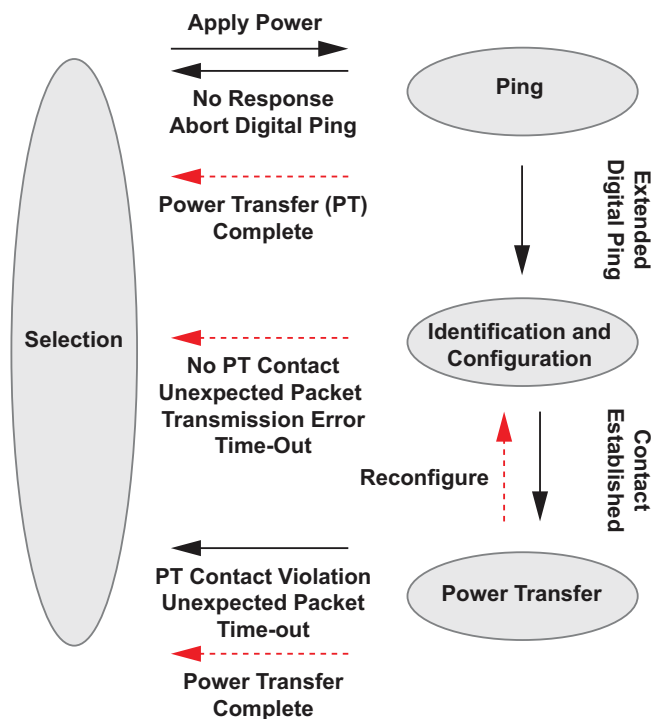


Figure 25 – WPC communication protocol.

A fixed clock frequency of approximately 2 kHz and a start bit is used before each 8-bit transmission, followed by parity and stop bits. The communications packet consists of four specific sections (preamble, header, message field and checksum) with the most common messages being:

- 1) Signal strength: Helps align the RX unit on the charging pad.
- 2) Control error packet: A signed integer value (–128 to +127) that represents the degree of error between the voltage at the RX LDO and its required voltage. In response, the TX adjusts its operating frequency using a proportional integral differential algorithm (PID). In steady-state, error packets are updated every 250 ms, but under a load step when a large error exists, the RX sends error packets at a faster rate of approximately 32 ms.
- 3) End power transfer packet: RX request instructing the TX to terminate power. Typically this is due to a fault condition or if the RX no longer requires power, for example, when the RX device's battery has been fully charged.

- 4) Rectified power packet: This is an unsigned integer value that communicates the amount of power the RX sees at the output of the rectifier circuit and is used in assessing coupling efficiency, maximum power limit and FOD. The TX terminates power transfer when no packets are received for a fixed interval of 350 ms minimum or 1800 ms maximum, indicating that a RX device is not present [20].

C. Equipment Needed to Advance a WPT

To close out this discussion, this paper examines the circuit behavior of a 5 W WPC compliant solution on the bench. The optimization of a wireless power solution necessitates tools for measuring complex impedances and circuit behavior. As such, a vector network analyzer (VNA) is an invaluable tool for building an understanding of a coil pair and modeling circuit behavior. Having a scope with a built-in spectrum analyzer is also helpful in assessing losses and EMI harmonic content. For this paper, a Bode 100 network analyzer capable of 40 MHz measurements and a mixed domain MDO4104 scope with integrated spectrum analyzer is used. A set of E-field and H-field probes [21] is used with the MDO4104 to evaluate radiated emissions. A non-contact IR imager or IR probe is also necessary when considering battery thermal coupling between the TX coil power losses and the portable electronic device.

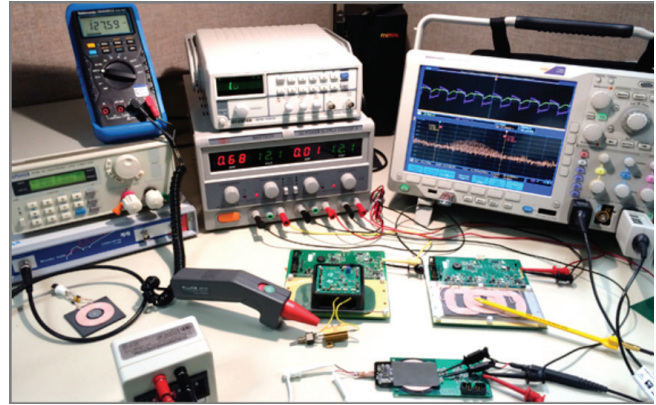
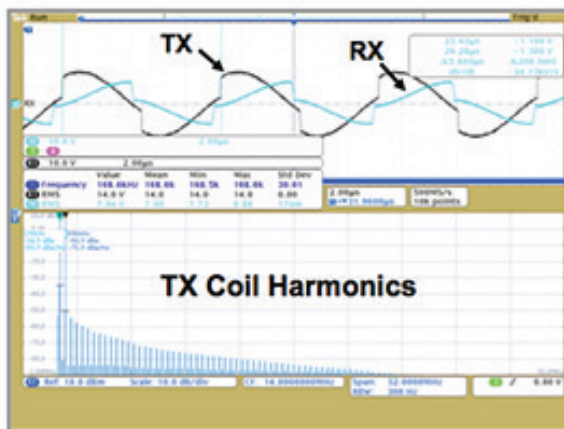


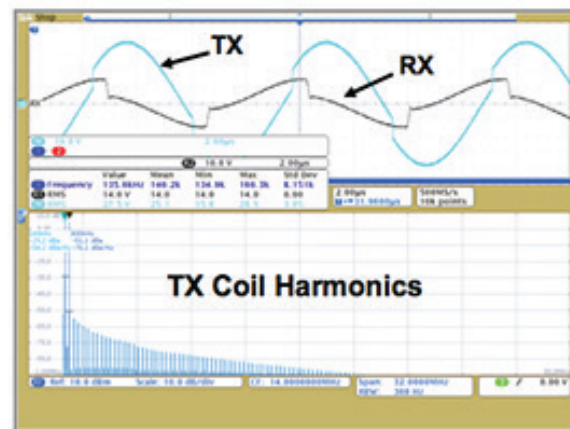
Figure 26 – Bench equipment and setup.

D. Coil Voltages and Harmonic Content – 5 W, WPC

Figure 27 is a scope plot of the TX/RX voltages and coil harmonics measured with an E-field probe. With the RX/TX coils in good alignment the TX voltage measures to be 20 Vpp and pseudo-sinusoidal and the RMS gain between the TX and RX calculates to be 0.56. Notice that when the TX moves to its maximum misalignment point the voltage nearly doubles to 40 Vpp and the gain drops to 0.509. Notice also that although the TX coil voltage does appear more sinusoidal there is little, if any, reduction in the resulting E-field harmonic content.



Centered coils force operation
further from resonance
 $V_{pp_tx} = 20 \text{ V}$, $f_{SW} = 170 \text{ kHz}$
RMS gain = 0.56



Misaligned coils force
operation closer to resonance
 $V_{pp_tx} = 40 \text{ V}$, $f_{SW} = 135 \text{ kHz}$
RMS gain = 0.509

Figure 27 – TX and RX coil voltage and harmonic content.

E. Intelligent Voltage Positioning

Figure 28 illustrates the behavior of a bqTesla™ receiver to intelligently position the rectified input voltage to the LDO thereby improving power converter efficiency and transient response. The RX sends load modulated error packets to the TX controller over the same power path as the reflected voltage and/or current to facilitate closed loop operation. To maintain good load regulation the TX responds by adjusting the input to a post regulator LDO. When the output is lightly loaded, the RX sends a control error packet (red trace) to increase the rectified input voltage (blue). Since the load current is light, the input-to-output differential voltage across the LDO does not represent significant power loss. The rectified level is set higher at light loads to accommodate the relatively slow digital communication loop and position the rectified voltage at a level to support the load under a low-to-high current transient (green trace). When steady-state is achieved the RX sends error packets back to the TX to minimize the differential voltage across the LDO. For example, at the maximum load current of 1.0 A, the rectified voltage is set to approximately 5.20 V.

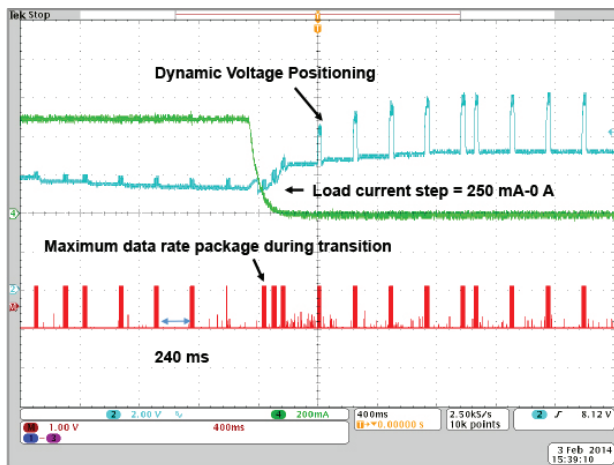


Figure 28 – Intelligent voltage positioning in response to a load step.

F. Transient Load Step Response

Now it is time to examine how an off-the-shelf WPC solution responds to a high current 1 A load step. Note that the time scale in Figure 29 is 100 ms per division. Two transmitters were used for

this measurement, one based on a 12 V, ½ bridge and another based on a 5 V full bridge. The load response in Figure 29 is nearly independent of the transmitter and the voltage drops from 5 V to 4 V, requiring multiple communication packets and nearly 700 ms to recover to the regulation point.

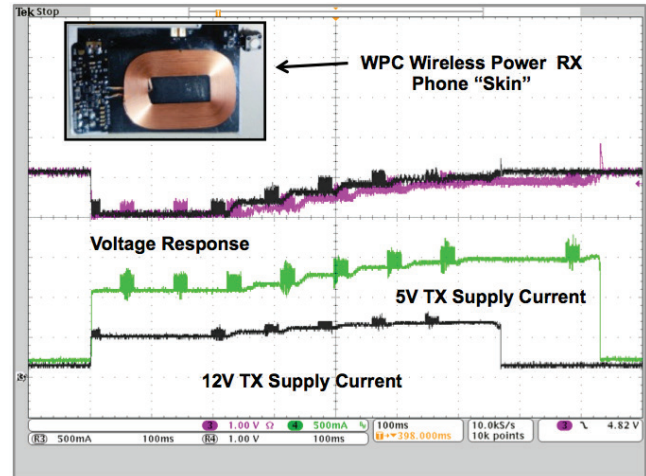


Figure 29 – Transient load step response – 1 A load step.

The green and black traces represent the TX current and the black and purple curves represent the output voltage response. Notice that packets of information being transmitted to the TX effectively modulate the load. After approximately seven packets of information (about 600 ms) the input voltage to the RX has been increased sufficiently to regulate at 5 V. The 250 mA load step response in Figure 30 is representative of a load step where a TX power correction packet is not necessary. As such the load step behavior is representative solely of the integrated post regulator LDO. The RX is removed from the phone sleeve; both the control circuitry and coil are fabricated onto a flex PCB. The design uses the TI WPC compliant bq51013B receiver IC. The 45 mm transmitter coil is driven by a soon-to-release and highly integrated coil driver IC that interfaces with a system μP . A very fast 1 A/ μs pulse is applied at the load and the response is illustrated in Figure 30.

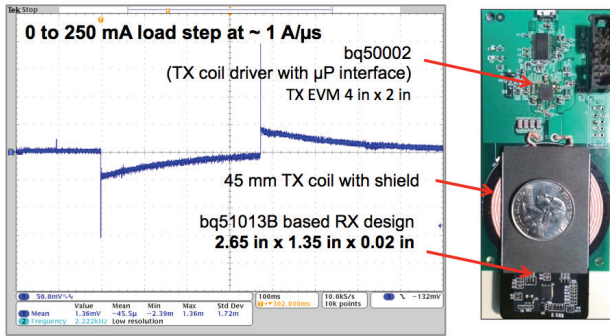


Figure 30 – 250 mA load step with the two chip TX solution.

G. Electromagnetic Compatibility

As with all power conversion, achieving an EMI compliant wireless power solution necessitates careful attention to parasitic board resonances as well as the resonant tank layout. Although a wireless power converter is a resonant converter topology with sinusoidal waveforms the coil voltage waveforms are typically pseudosinusoidal and rich in E-field harmonic content. As such, pay careful attention to board parasitics, field surfaces and layout loop area. To address E-field radiated emissions off the TX coil a “finger shield” is constructed to shunt the radiated E-field

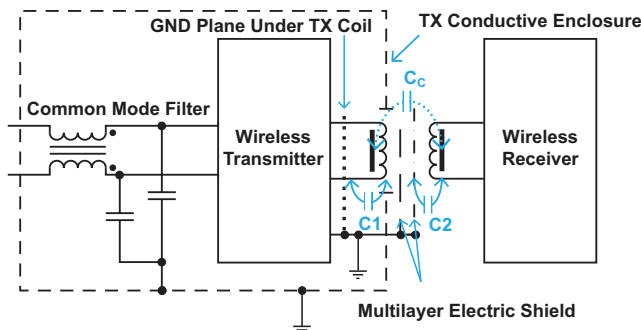


Figure 31 – EMI mitigation using a CM choke and “finger shield”.

to ground where it can be addressed by a common-mode choke. Snubbers and shielding are also commonly required. The constructed shield uses a PCB with interleaved, thin copper strips that act as a solid shield with minimal eddy losses [20]. The shield significantly reduces radiated emissions by as much as 20 dB with minimal impact on efficiency.

H. Foreign Object Detection

Leakage flux near the power transfer edges couples into foreign objects and, depending on the specific heat of the material, quickly results in unsafe temperatures. In particular, the battery must be shielded from this leakage flux to avert potentially catastrophic conditions – just 0.5 W of induced losses in 1 g of silver results in a 75 °C rise in temperature in 15 s. To mitigate a potentially unsafe condition, foreign object detection is necessary and required by all standards. As indicated earlier, the RX reports its received power and the TX constantly monitors its losses. Figure 32 illustrates how loss accounting in a wireless power transfer responds to induced losses by foreign objects. A software tool was developed for this purpose and an experiment constructed. Figure 32 shows the results where an artificially high fault threshold (1.9W FOD induced loss) is selected to ensure constant power transfer while the foreign object is present; typically once the threshold is exceeded power transfer is interrupted. At time = 0 an alligator clip is placed adjacent to a 5 W field of misaligned coils. As stated earlier near-field inductive energy is conserved unless intercepted by a coil or metallic surface, in this case the alligator clip. The misalignment of the coils creates a flux area where foreign objects are introduced. The additional losses in the alligator clip measure 1.36 W and the object reaches 55 °C in under 60 s. When the object is removed, the reported losses drop to less than 100 mW. This kind of intelligent loss reconciliation is a safety consideration that must be integrated into any WPT solution.

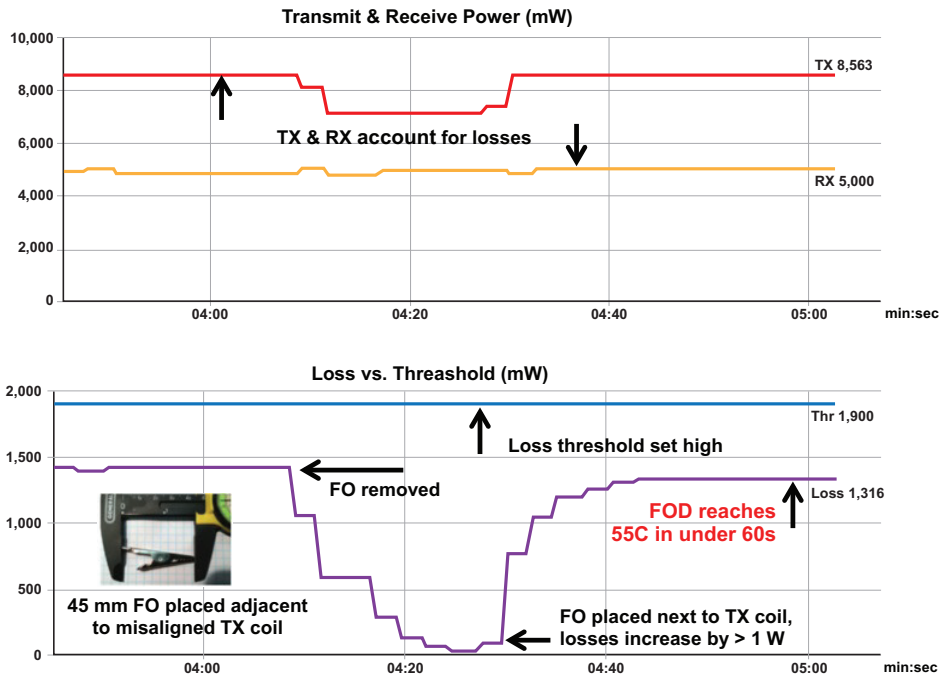


Figure 32 – Loss reconciliation between TX and RX.

IV. CONCLUSION

Wireless power transfer is a technology positioned to be as ubiquitous as the cell phones people depend on. Whether an internet-connected cell phone, wearable fitness device or other battery operated device, wireless power makes charging devices more convenient and, in some cases, safer too. Does WTP represent a more or less efficient solution? Well, that depends. An intelligent TX can operate in many modes, for example turning off once a battery is charged, rather than dwelling in some higher power-dissipating state. When thinking about the number of wired power adaptors operating overnight in a typical household, WTP certainly could translate into a greener overall solution.

For the 5-15 W use case, there is little questioning that wireless power with MR/MI makes sense in many applications and it is already positioned for wide deployment. What about charging your laptop battery at 45 W from across the room? Well, there are issues to resolve here, most notably power transfer efficiency and the associated health implications. Lastly there are the high power applications for battery electric vehicles and buses. Again, application and infrastructure challenges are there, but in the

isolated region under a car a TX/RX coil pair that is separated by 20-30 cm is not burdened by the same field strength implications and therefore is more readily imagined.

In a world fitted with battery-operated portable electronics and wireless communication, intelligent wireless power facilitates convenience, eliminates the clutter of cables and connectors and creates an invisible power source well suited for charging batteries. A great deal of opportunity exists for innovation in the area of WPT for those able to imagine the possibilities and overcome the obstacles presented in this paper.

V. ACKNOWLEDGEMENTS

I would like to thank the entire wireless power develop team at TI including, but not limited to Steve Goacher, Kalyan Siddabattula, Steven Terry, Pearl Cao, Ashish Khandelwal and Eric Oettinger for their efforts in advancing this technology and support. I would also like to thank Tektronix and Bill Brady for his enthusiastic support and equipment that I needed to develop the paper. Lastly, I need to recognize my friend and co-worker Mike Segal of Texas Instruments for his continued encouragement and efforts in proof reading my paper and presentation.

VI. REFERENCES

- [1] Schneider, David. "A Critical Look at Wireless Power." IEEE Spectrum, Posted 30 Apr. 2010.
- [2] Barsukov, Yevgen. "Battery Selection, Safety, and Monitoring in Mobile Applications." Texas Instruments.
- [3] Miller, John M., Scudiere, Matthew B., McKeever and White, Cliff. "Wireless Power Transfer." Oak Ridge National Laboratory's Power Electronics Symposium.
- [4] Šarboh, Snežana. Sixth International Symposium Nikola Tesla. October, 2006, Belgrade, SASA, Serbia.
- [5] Capps, Charles. "Near Field or Far Field?" EDN, August 16, 2001, www.ednmag.com.
- [6] Beh, TeckChuan, Kato, Masaki, Imura, Takehiro, and Hori, Yoichi. "Wireless Power Transfer System via Magnetic Resonant - Coupling at Fixed Resonance Frequency --Power Transfer System Based on Impedance Matching." Nov 5-9, 2010, Department of Advanced Energy, Graduate School of Frontier Science.
- [7] Schoepges, Holger. "Wireless Energy Transmission: New Technology Will Soon Charge Smartphones in Cars." Press release. September 2013, CE4a.org, wirelesspowerconsortium.com.
- [8] BQ51221, Dual Mode 5-W (WPC and PMA) Single Chip Wireless Power Receiver. Accessed 7-18-2014. www.ti.com/lit/ug/sl000ax6b/sl000ax6b.pdf.
- [9] "Guidelines for Limiting Exposure to Time-Varying Electric, Magnetic, and Electromagnetic Fields." International Commission on Non-Ionizing Radiation Protection.
- [10] Kurs, André, Karalis, Aristeidis, Moffatt, Robert, Joannopoulos, J. D., Fisher, Peter, Soljačić, Marin. "Wireless Power Transfer via Strongly Coupled Magnetic Resonances." July 6, 2007, Sciencemag.org.
- [11] Waffenschmidt, Eberhard. "Resonant Coupling." wirelesspowerconsortium.com.
- [12] Liu, Xun, Ng, W.M, Lee, C.K. and Hui, S.Y. "Optimal Operation of Contactless Transformers with Resonance in Secondary Circuits." Center for Power Electronics, City University of Hong Kong.
- [13] Sandler, Steve and Hymowitz, Charles. "Optimize Wireless Power Transfer Link Efficiency." Sep 26, 2011, <http://powerelectronics.com/alternative-energy/optimize-wireless-power-transfer-link-efficiency-part-1>.
- [14] Deisch, Celic. "Modeling Skin Effect in Spice." September 28, 2006, ednmag.com.
- [15] Michael, Tse. "Impedance Matching." Hong Kong Polytechnic University, http://158.132.149.224/module/EIE574/download/FM_saveAs.php?filename=/impedancematching.pdf.
- [16] Kollman, Robert. "Convert Parallel Impedances to Series Impedances." Texas Instruments, June 21, 2010, EE Times magazine, http://www.eetimes.com/document.asp?doc_id=1278134.
- [17] See reference 6.
- [18] Rice, John, Gehrke, Dirk and Segal, Mike. "Understanding Noise-Spreading Techniques and Their Effects in Switch-Mode Power Applications." Texas Instruments Power Supply Design Seminar, http://www.ti.com/download/trng/docs/seminar/Topic_2_Rice_Gehrke_Segal.pdf.
- [19] FEMM Finite Element Analysis Software Homepage, <http://www.femm.info/wiki/HomePage>.
- [20] Sengupta, Upal and Johns, Bill. "Universally Compatible Wireless Power Using the Qi Protocol." Texas Instruments, http://www.low-powerdesign.com/article_TI-Qi.html.
- [21] Muratov, Vladimir A. and Rice, John C. "Wireless Power Transfer System With Reduced Electromagnetic Emissions." <http://www.google.com/patents/US20130181535>.

TI Worldwide Technical Support

Internet

TI Semiconductor Product Information Center Home Page

support.ti.com

TI E2E™ Community Home Page

e2e.ti.com

Product Information Centers

| | | |
|-----------------|----------------|--|
| Americas | Phone | +1(512) 434-1560 |
| Brazil | Phone | 0800-891-2616 |
| Mexico | Phone | 0800-670-7544 |
| | Fax | +1(972) 927-6377 |
| | Internet/Email | support.ti.com/sc/pic/americas.htm |

Europe, Middle East, and Africa

| | |
|--------------------|--------------------------------------|
| Phone | |
| European Free Call | 00800-ASK-TEXAS (00800 275 83927) |
| International | +49 (0) 8161 80 2121 |
| Russian Support | +7 (4) 95 98 10 701 |

Note: The European Free Call (Toll Free) number is not active in all countries. If you have technical difficulty calling the free call number, please use the international number above.

| | |
|--------------|--|
| Fax | + (49) (0) 8161 80 2045 |
| Internet | www.ti.com/asktexas |
| Direct Email | asktexas@ti.com |

Japan

| | | |
|----------------|---------------|--|
| Phone | Domestic | 0120-92-3326 |
| Fax | International | +81-3-3344-5317 |
| | Domestic | 0120-81-0036 |
| Internet/Email | International | support.ti.com/sc/pic/japan.htm |
| | Domestic | www.tij.co.jp/pic |

Asia

Phone Toll-Free Number
Note: Toll-free numbers may not support mobile and IP phones.

| | |
|-------------|-------------------|
| Australia | 1-800-999-084 |
| China | 800-820-8682 |
| Hong Kong | 800-96-5941 |
| India | 000-800-100-8888 |
| Indonesia | 001-803-8861-1006 |
| Korea | 080-551-2804 |
| Malaysia | 1-800-80-3973 |
| New Zealand | 0800-446-934 |
| Philippines | 1-800-765-7404 |
| Singapore | 800-886-1028 |
| Taiwan | 0800-006800 |
| Thailand | 001-800-886-0010 |

| | |
|---------------|--|
| International | +86-21-23073444 |
| Fax | +86-21-23073686 |
| Email | tiasia@ti.com or ti-china@ti.com |
| Internet | support.ti.com/sc/pic/asia.htm |

Important Notice: The products and services of Texas Instruments Incorporated and its subsidiaries described herein are sold subject to TI's standard terms and conditions of sale. Customers are advised to obtain the most current and complete information about TI products and services before placing orders. TI assumes no liability for applications assistance, customer's applications or product designs, software performance, or infringement of patents. The publication of information regarding any other company's products or services does not constitute TI's approval, warranty or endorsement thereof.

A012014

The platform bar and E2E are trademarks of Texas Instruments. All other trademarks are the property of their respective owners.

IMPORTANT NOTICE

Texas Instruments Incorporated and its subsidiaries (TI) reserve the right to make corrections, enhancements, improvements and other changes to its semiconductor products and services per JESD46, latest issue, and to discontinue any product or service per JESD48, latest issue. Buyers should obtain the latest relevant information before placing orders and should verify that such information is current and complete. All semiconductor products (also referred to herein as "components") are sold subject to TI's terms and conditions of sale supplied at the time of order acknowledgment.

TI warrants performance of its components to the specifications applicable at the time of sale, in accordance with the warranty in TI's terms and conditions of sale of semiconductor products. Testing and other quality control techniques are used to the extent TI deems necessary to support this warranty. Except where mandated by applicable law, testing of all parameters of each component is not necessarily performed.

TI assumes no liability for applications assistance or the design of Buyers' products. Buyers are responsible for their products and applications using TI components. To minimize the risks associated with Buyers' products and applications, Buyers should provide adequate design and operating safeguards.

TI does not warrant or represent that any license, either express or implied, is granted under any patent right, copyright, mask work right, or other intellectual property right relating to any combination, machine, or process in which TI components or services are used. Information published by TI regarding third-party products or services does not constitute a license to use such products or services or a warranty or endorsement thereof. Use of such information may require a license from a third party under the patents or other intellectual property of the third party, or a license from TI under the patents or other intellectual property of TI.

Reproduction of significant portions of TI information in TI data books or data sheets is permissible only if reproduction is without alteration and is accompanied by all associated warranties, conditions, limitations, and notices. TI is not responsible or liable for such altered documentation. Information of third parties may be subject to additional restrictions.

Resale of TI components or services with statements different from or beyond the parameters stated by TI for that component or service voids all express and any implied warranties for the associated TI component or service and is an unfair and deceptive business practice. TI is not responsible or liable for any such statements.

Buyer acknowledges and agrees that it is solely responsible for compliance with all legal, regulatory and safety-related requirements concerning its products, and any use of TI components in its applications, notwithstanding any applications-related information or support that may be provided by TI. Buyer represents and agrees that it has all the necessary expertise to create and implement safeguards which anticipate dangerous consequences of failures, monitor failures and their consequences, lessen the likelihood of failures that might cause harm and take appropriate remedial actions. Buyer will fully indemnify TI and its representatives against any damages arising out of the use of any TI components in safety-critical applications.

In some cases, TI components may be promoted specifically to facilitate safety-related applications. With such components, TI's goal is to help enable customers to design and create their own end-product solutions that meet applicable functional safety standards and requirements. Nonetheless, such components are subject to these terms.

No TI components are authorized for use in FDA Class III (or similar life-critical medical equipment) unless authorized officers of the parties have executed a special agreement specifically governing such use.

Only those TI components which TI has specifically designated as military grade or "enhanced plastic" are designed and intended for use in military/aerospace applications or environments. Buyer acknowledges and agrees that any military or aerospace use of TI components which have **not** been so designated is solely at the Buyer's risk, and that Buyer is solely responsible for compliance with all legal and regulatory requirements in connection with such use.

TI has specifically designated certain components as meeting ISO/TS16949 requirements, mainly for automotive use. In any case of use of non-designated products, TI will not be responsible for any failure to meet ISO/TS16949.

Products

| | |
|------------------------------|--|
| Audio | www.ti.com/audio |
| Amplifiers | amplifier.ti.com |
| Data Converters | dataconverter.ti.com |
| DLP® Products | www.dlp.com |
| DSP | dsp.ti.com |
| Clocks and Timers | www.ti.com/clocks |
| Interface | interface.ti.com |
| Logic | logic.ti.com |
| Power Mgmt | power.ti.com |
| Microcontrollers | microcontroller.ti.com |
| RFID | www.ti-rfid.com |
| OMAP Applications Processors | www.ti.com/omap |
| Wireless Connectivity | www.ti.com/wirelessconnectivity |

Applications

| | |
|-------------------------------|--|
| Automotive and Transportation | www.ti.com/automotive |
| Communications and Telecom | www.ti.com/communications |
| Computers and Peripherals | www.ti.com/computers |
| Consumer Electronics | www.ti.com/consumer-apps |
| Energy and Lighting | www.ti.com/energy |
| Industrial | www.ti.com/industrial |
| Medical | www.ti.com/medical |
| Security | www.ti.com/security |
| Space, Avionics and Defense | www.ti.com/space-avionics-defense |
| Video and Imaging | www.ti.com/video |

TI E2E Community

e2e.ti.com